Formulation and assessment of flamelet-generated manifolds for reacting interfaces

Brian T. Bojko, Paul E. DesJardin*

Department of Mechanical and Aerospace Engineering, University at Buffalo, the State University of New York, Buffalo, NY 14260-4400, United States

A B S T R A C T

The coupling of heat and mass transfer at the surface of solid or liquid fuels is important when modeling near-surface gasification and combustion processes. Modeling the reacting boundary layer with the use of finite-rate chemistry allows for a highly accurate description of the coupling between the flame and fuel surface, but is not tractable when considering detailed chemical kinetic mechanisms. In this study, simplified unsteady 1D flames with mass blowing are considered for a solid biomass fuel where the flamelet-generated manifold (FGM) method is employed as a model reduction strategy for potential application to multidimensional calculations, such as flame spread over solid materials undergoing pyrolysis and ablation. Two types of FGM are considered. The first are a set of steady-state flames differentiated by their scalar dissipation rate. Steady flamelets have been used extensively in the past for jets, shear-layers, *etc.* but, their application to solid fuel boundaries is new. Results show that the use of steady flames produce unacceptable errors, with temperature errors in excess of 45%. To avoid these errors, a new methodology for developing an unsteady FGM is presented that accounts for unsteady diffusion effects but, is also independent of surface mass flux. Results using the unsteady FGM greatly reduces errors in temperature with differences that are under 10%.

© 2016 The Combustion Institute. Published by Elsevier Inc. All rights reserved.

1. Introduction

The flamelet-generated manifold (FGM) [1–3] method has been used to describe premixed flames [4,5] and non-premixed flames [3,6] with extensions to multi-dimensional turbulent combustion environments. Recently, Knudsen and Pitsch [7] have studied the combination of premixed and non-premixed flamelets to assess their mutual application to describe partially-premixed combustion environments. Wu et al. [8] introduced the Pareto-efficient combustion model for predicting and modeling multi-regime flames. Vreman et al. [9] and Ihme et al. [10] have successfully applied the FGM method to complex turbulent combustion simulations of the experimental set of Sandia D and E flames developed by Barlow et al. [11]. The FGM approach has also been extended to modeling dilute spray combustion including *n*-heptane [12], α-methylnaphthalene/*n*-decane [13], *n*-dodecane [14], acetone sprays [15], and Jet-A fuel [16].

Reacting boundary layers of solid/liquid fuels requires an accurate description of the surface heat flux in order to sufficiently model the coupling of heat and mass transfer at the surface under-going gasification as well as, for determining the resulting flame configuration. The mass flux at the solid/liquid surface can result in unsteady diffusion flames in multidimensional burning configurations such as upward flame-spread and burning propellant in solid rockets. For this class of flames, Xie and DesJardin developed an embedded flame modeling approach where the governing equations for the conjugate heat and mass transfer between a solid and fluid interface are described [17]. The coupling method was applied to DNS of upward flame spread of solid poly(methyl methacrylate) (PMMA) undergoing pyrolysis [18]. Model reduction of the DNS results were conducted to reduce the degrees of freedom of the problem, but rely on collapsing the entire DNS solution to generate the reduced lookup table. The FGM has an advantage in that it maintains generality by storing the finite-rate chemistry source terms of individual flames instead of needing multiple, particular flame spread solutions to generate the manifold. The goal of this study is to extend the work of Xie and DesJardin by investigating the application of flamelet-generated manifolds for solid biomass combustion with constant mass blowing through the assessment of a steady and unsteady FGM approach.

The rest of this study is organized as follows. In Section 2.1, the governing equations and boundary conditions for the 1D reacting boundary layer are presented. Section 2.2, describes how the boundary conditions are determined through the use of a

---

* Corresponding author.
 E-mail addresses: btbojko@gmail.com (B.T. Bojko), ped3@buffalo.edu (P.E. DesJardin).

multiphase equilibrium solver to evaluate pyrolysis species composition of the solid fuel. In Sections 3.1 and 3.2, two FGM modeling methodologies are presented. The first is a steady FGM approach constructed from the steady-state 1D diffusion flame solutions. The second approach uses unsteady diffusion flame solutions to create the unsteady FGM method. Results of the exact solution to the 1D reacting boundary layer are presented in Section 4.1. Validation of the steady FGM approach without mass blowing is conducted in Section 4.2, and then comparisons of the steady and unsteady FGM are made to the exact solution of 1D flames with mass blowing. Finally, conclusions are drawn on the application of steady and unsteady FGM.

2. Problem description

2.1. Reacting boundary in 1D

The gas phase solution is considered one-dimensional, fully compressible and viscous, resulting in the following set of conservation equations for mass, species, momentum and energy,

$$\frac{\partial \rho}{\partial t} + \frac{\partial (\rho u_x)}{\partial x} = 0 \tag{1a}$$

$$\frac{\partial (\rho Y_i)}{\partial t} + \frac{\partial (\rho u_x Y_i)}{\partial x} = \frac{\partial}{\partial x}\left(\rho D_i \frac{\partial Y_i}{\partial x}\right) + \dot{w}_i \tag{1b}$$

$$\frac{\partial (\rho u_x)}{\partial t} + \frac{\partial (\rho u_x^2)}{\partial x} = -\frac{\partial p}{\partial x} + \frac{\partial}{\partial x}\left(\mu \frac{\partial u_x}{\partial x}\right) \tag{1c}$$

$$\frac{\partial (\rho e_t)}{\partial t} + \frac{\partial}{\partial x}(\rho u_x H_t) = \frac{\partial}{\partial x}\left(u_x \mu \frac{\partial u_x}{\partial x}\right)$$
$$+ \frac{\partial}{\partial x}\left(k\frac{\partial T}{\partial x} + \sum_i^N \rho D_i \frac{\partial Y_i}{\partial x}h_i\right) - \sum \dot{w}_i h_{f,i}^o \tag{1d}$$

where, $\dot{w}_i$ is the mass consumption or production rate of the ith species, $e_t (= e + u_x^2/2)$ is the total sensible energy, $H_t (= e_t + p/\rho)$ is the total enthalpy, and $h_{f,i}^o$ is the heat of formation of the ith species. Assuming constant diffusivity, it can be shown [19] that, $\left(k\frac{\partial T}{\partial x} + \sum_i^N \rho D_i \frac{\partial Y_i}{\partial x}h_i\right)$, can be expressed as,

$$\mu \frac{c_p}{Pr}\left(1 - \frac{1}{Le}\right)\frac{dT}{dx} + \frac{1}{Sc}\frac{dh}{dx} \tag{2}$$

where, Pr is the Prandtl number, Sc is the Schmidt number, Le is the Lewis number, and h is the sensible enthalpy. Although differential diffusion is important, it has been neglected here to maintain a one-to-one correlation between the exact solution and transport equations for Z and C when comparing to the FGM implementation and to simplify the interpretation of results. Prandtl (Pr) and Schmidt (Sc) numbers are both set equal to 0.707, resulting in a unity Lewis number assumption. Viscosities are determined from the Sutherland viscosity model, while thermal and molecular diffusivities are calculated using the definitions of Pr and Sc respectively. Molecular fluxes are approximated using a second-order centered differencing approach, employing a semi-implicit operator to avoid diffusion time step stability limitations. The boundary conditions for the mass, species, and energy are explicitly set at the surface by imposing a total convective mass flux and specifying the species mass fractions and temperature at the solid/gas interface. Species and temperature at the surface are determined from a multiphase chemical equilibrium solution and mass fluxes are set to values typical of biomass combustion, to be discussed.

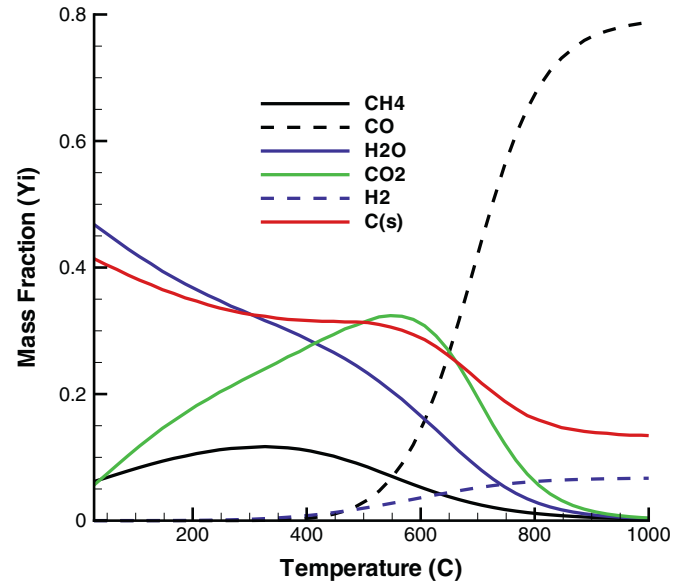A finite volume method is used to solve the coupled system of non-linear equations and a second-order fractional step

Fig. 1. Equilibrium composition of major species for wood undergoing pyrolysis at various temperatures.

method is used to integrate the equations using a two-stage Runge–Kutta time integration. Convective fluxes are discretized using an AUSM+UP flux vector splitting [20] with a combination of second-order upwind biased and essentially non-oscillatory (ENO) interpolants for determining fluxes [21,22]. The GRI-Mech 3.0 [23], consisting of 53 species and 325 reactions, is used to describe the combustion of pyrolysis gases, which is an appropriate choice considering the primary combustibles are CH_4 and CO. While the kinetic mechanism is not specifically tailored for biomass decomposition into tar and char, the objective of this study is to assess the FGM method applied to biomass-like combustion and is expected to be insensitive to these assumptions.

2.2. Fuel boundary

To determine the values of $Y_{i,s}$ at the fuel boundary a local multiphase chemical equilibrium is assumed. For this study, the interest lies in the solid biomass combustion of wood, where the fuel is assumed to be composed of, $CH_{1.7}O_{0.72}N_{0.001}$. A one-step atomic balance is used to estimate the chemical decomposition of the solid fuel into a set of realizable species expressed as,

$$CH_{1.7}O_{0.72}N_{0.001} \rightarrow 0.28\,CH_4 + 0.36\,CO + 0.29\,H_2$$
$$+ 5 \times 10^{-4}\,N_2 + 0.36\,O + 0.36\,C(s) \tag{3}$$
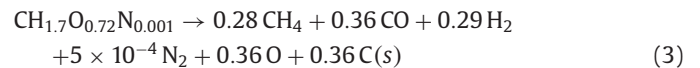
where, thermodynamic properties are readily available for the species on the R.H.S. of Eq. (3). This composition is used as an input into a multiphase equilibrium solver using a Gibbs minimization procedure and elemental conservation which is solved using an algorithm similar to that in STANJAN [24].

Figure 1 shows pyrolysis products as a function of temperature. The char yield is estimated by $C(s)$, when this value plateaus at 31.5% for temperatures between $300\,^{\circ}C$ and $550\,^{\circ}C$ is when the main pyrolysis event occurs, consistent with values reported in the literature from thermal degradation experiments conducted with a batch reactor [25]. As the temperature increases further beyond $550\,^{\circ}C$, the CO_2 begins to decompose and the major species within the pyrolysis gases transitions to carbon-monoxide. Using the center of the region where the 31.5% char yield is constant to define the active gasification region, the pyrolysis temperature, $T_s = T_{pyr}$, is chosen to be $425\,^{\circ}C$ (700 K) and is typical of reported pyrolysis temperatures [26,27]. At this temperature the major